

# Modeling Dynamic Signatures through Two-Link Robotic Arm Biomechanics with Torque Features and CNN–BiLSTM for Forgery Detection

<sup>1</sup> Atiya Kazi, <sup>2</sup> Dr. Vinayak Bharadi, <sup>3</sup> Dr. Kaushal Prasad

<sup>1,2,3</sup> Department of Information Technology,

<sup>1,2,3</sup> Finolex Academy of Management and Technology,

<sup>1,2,3</sup> Ratnagiri, India

<sup>1</sup> *atiya.kazi@famt.ac.in*, <sup>2</sup> *vinayak.bharadi@famt.ac.in*, <sup>3</sup> *kaushal.prasad@famt.ac.in*

**Abstract**—Dynamic signature verification remains a challenging biometric problem due to the subtle neuromotor variations that differentiate genuine handwriting from skilled forgeries. This work introduces a biomechanics-inspired approach that models the human signing process as a two-link robotic arm, enabling the extraction of joint-space kinematic and torque-driven dynamic features from standard pen-trajectory data. Raw signature coordinates from the SVC2004 Task-2 dataset are first normalized and transformed into joint angles using inverse kinematics. Angular velocities, angular accelerations, and torque estimates are then derived through numerical differentiation, creating a six-dimensional temporal representation that captures the underlying neuromotor effort exerted during writing. These torque-enhanced sequences are fed into a hybrid deep learning framework combining one-dimensional CNN layers for local pattern extraction with a bidirectional LSTM network for temporal dependency modelling. The proposed system is trained using an 80/20 stratified split and evaluated using classification and verification metrics. Experimental results demonstrate strong discrimination between genuine signatures and skilled forgeries, confirming that torque-based biomechanical cues encode writer-specific motion dynamics not evident in spatial trajectory features alone. This study establishes two-link robotic arm biomechanics as an effective modelling paradigm for dynamic signatures and highlights torque-driven features as a promising direction for next-generation biometric authentication systems.

**Index Terms**—Dynamic Signature Verification, Biomechanics, Two-Link Robotic Arm Model, Torque-Based Features, Inverse Kinematics, Neuromotor Dynamics, CNN–BiLSTM, Deep Learning, Skilled Forgery Detection, Online Handwriting Biometrics.

## I. INTRODUCTION

Dynamic Signature Verification (DSV) is a behavioural biometric technique that analyses the temporal patterns of handwriting to authenticate an individual. Unlike static signatures, dynamic signatures incorporate information such as pen trajectory, velocity, timing, and pressure, making them rich in neuromotor cues and inherently more resistant to forgery. With the increasing adoption of digital devices capable of capturing fine-grained handwriting data, DSV has become a reliable component in secure identity verification systems used in banking, legal documentation, and digital transactions. Most existing DSV systems rely on features extracted directly from the Cartesian trajectory of the pen. Traditional methods use handcrafted features such as velocity profiles, curvature, and pen-up/down transitions, while modern deep learning approaches learn spatial–temporal representations directly from raw (X, Y, Time) sequences. Although these approaches have demonstrated promising results, they share a common limitation: they model only the external movement of the pen tip and overlook the internal biomechanical processes that generate the signature. Skilled forgers often mimic the visible trajectory closely, making trajectory-only systems susceptible to sophisticated imitation attacks. Human handwriting originates from coordinated neuromotor activity across joints in the fingers, wrist, and arm. The visible pen trajectory represents only the final outcome of this internal motion. The biomechanical effort required to produce a signature—including joint rotation, muscular control, and movement torque—is difficult for a forger to replicate, even when the traced path is visually similar. This motivates a deeper modelling approach that interprets handwriting not merely as a two-dimensional trace but as the result of joint-level dynamics generated by the human motor system. In this study, dynamic signatures are modeled as the end-effector motion of a two-link robotic arm to reconstruct the underlying joint behaviour involved in writing. Using inverse kinematics, each point in the pen trajectory is mapped to estimated joint angles, enabling the computation of angular velocities, angular accelerations, and torque profiles. These torque-based biomechanical features reveal neuromotor patterns that remain hidden in trajectory-only analysis. Skilled forgeries may approximate the pen path but cannot imitate the internal joint dynamics or torque signatures that reflect genuine motor control characteristics. To learn discriminative patterns from these biomechanical sequences, a hybrid deep learning framework combining one-dimensional Convolutional Neural Networks (CNNs) and Bidirectional Long Short-Term Memory (BiLSTM) networks is employed. The CNN layers extract localized temporal variations from torque and joint dynamics, while the BiLSTM layers model long-range dependencies across the entire signature. This integration produces a robust representation capable of distinguishing genuine signatures from skilled forgeries with higher reliability.

### 1.1 Novelty of the Study

- Introduces a biomechanics-inspired modelling approach that represents dynamic signatures as the end-effector motion of a two-link robotic arm, moving beyond traditional Cartesian trajectory analysis.
- Applies inverse kinematics to reconstruct joint angles for every point in the pen trajectory, providing access to the internal joint behaviour behind handwriting rather than only the visible path.
- Derives angular velocities, angular accelerations, and torque profiles, capturing neuromotor effort and biomechanical characteristics that are extremely difficult for skilled forgers to imitate.
- Proposes torque-driven joint dynamics as a new and previously unexplored feature domain for Dynamic Signature Verification, expanding beyond conventional kinematic and pressure-based features.
- Integrates these biomechanics-based features with a hybrid CNN–BiLSTM network, enabling effective learning of both local temporal variations and long-range dependencies within the signature.
- Demonstrates that torque-enhanced representations significantly improve the discrimination between genuine signatures and skilled forgeries compared to trajectory-only deep learning models.
- Establishes a unified framework that combines inverse kinematics, torque computation, temporal feature modeling, and deep classification for a more robust, forgery-resistant signature verification system.

### 1.2 Research Gaps Addressed

- Existing DSV systems primarily rely on Cartesian trajectory features and overlook the biomechanical processes that generate handwriting, limiting their ability to capture neuromotor behaviour.
- Current deep learning models focus on spatial–temporal learning from raw (X, Y, Time) data but do not incorporate joint angles, torques, or biomechanical cues that offer deeper writer-specific information.
- Skilled forgery detection remains challenging because forgers can mimic the visual shape of a signature but cannot reproduce the internal joint dynamics, which are not exploited in existing DSV approaches.
- No prior work models handwriting as a two-link arm system or computes torque-based neuromotor signatures derived from inverse kinematics.
- The fusion of biomechanics-driven features with CNN–BiLSTM architectures is underexplored, leaving a gap in combining physics-based modeling with deep sequence learning.
- A unified pipeline integrating inverse kinematics, dynamic torque computation, and deep temporal classification has not been previously developed for signature verification.

## II. RELATED WORK

Dynamic modeling of human movement and robotic biomechanics has been widely explored for torque estimation, motion optimization, and adaptive control. Studies such as Shakeriaski and Mohammadian [1] have leveraged deep learning for torque prediction in exoskeletons, using BiLSTM architectures to model nonlinear dynamics of upper-limb motion. While effective for rehabilitation robotics, their approach focuses primarily on assistive control rather than capturing fine neuromotor variations associated with individual handwriting signatures. Similarly, Zhu et al. [2] optimized two-link robotic arms through simultaneous control and structural parameter tuning, but did not extend their framework to model human-like biomechanical variability essential for biometric applications. Several researchers have investigated torque-based control and adaptive schemes for two-link robotic systems. Nguyen [3], [7] introduced sliding mode and fractional-order controllers for joint torque regulation, achieving improved response and robustness under nonlinear dynamics. These contributions highlight the value of torque features in dynamic modeling but are limited to mechanical control precision rather than cognitive or neuromotor expression as seen in signature dynamics. Ogura and Aoki [4] simulated bi-articular muscle effects using torque-driven flexible joints, establishing parallels with human motor control; however, they did not exploit these signals for identity recognition tasks. From a control systems standpoint, torque-based optimization has been extensively applied in classical and hybrid schemes. Works by Shah and Rattan [5] and Feddema et al. [6] demonstrated torque-controlled trajectory tracking and sensor-based feedback in flexible two-link arms. Similarly, Lucibello and Bellezza [11] proposed nonlinear adaptive control to maintain stability under payload variations. While these studies contributed to accurate dynamic modeling, they lack a high-level feature representation necessary for pattern recognition tasks such as biometric forgery detection. Research into torque dynamics near singular configurations [8]–[10] revealed that energy efficiency and motion adaptability can be optimized by exploiting biomechanical singularities. These insights provide an important foundation for representing the neuromotor characteristics of handwriting motions, where small changes in angular dynamics produce distinct torque signatures. Nonetheless, these studies did not explore how such biomechanical principles could enhance dynamic signature verification systems. On the other hand, advances in data-driven learning have demonstrated the power of hybrid deep models in understanding complex motor sequences. The Glove-Net framework by Pratap et al. [2nd ref—Sensors 2024] employed CNN–BiLSTM fusion to classify human grasp patterns using temporal and force data. This architecture effectively integrates spatial–temporal dependencies, making it highly suitable for analyzing dynamic handwriting trajectories. However, their application domain was limited to object grasp recognition, and the input modality excluded torque-derived biomechanical cues. In addition, simulation-based studies [12]–[14] on computed torque control, dynamic modeling, and system identification confirm that torque–angle coupling captures critical dynamic patterns. Bolignari et al. [15] extended this line of research to develop human-friendly robotic arms capable of real-time torque sensing and compliant motion. Despite progress in torque measurement and modeling, none of these

frameworks have been explicitly adapted to detect fine-grained forgeries in dynamic signature data, where subtle neuromotor deviations are crucial.

## 2.1 Research Gaps Identified

### 1. Lack of biomechanical representation in signature verification:

Existing deep learning approaches to signature verification primarily rely on trajectory or velocity data, ignoring torque-based neuromotor features that encode individual motor effort [1], [3], [4], [5].

### 2. Absence of hybrid spatial–temporal learning on torque sequences:

Prior torque modeling research has not integrated deep sequence networks like CNN–BiLSTM to extract hierarchical temporal dependencies from torque signals [2], [7], [11].

### 3. Disconnection between robotic biomechanics and biometrics:

While torque-driven robotic arm models exist, they have not been applied to biometric problems where microdynamics of motion (e.g., signing) are indicative of identity [4], [8], [10].

### 4. Limited interpretability of dynamic features:

Existing signature verification systems often employ black-box feature extraction methods that do not link the features to physiological or neuromotor origins [1], [9], [12].

## 2.2 Proposed Framework Contribution

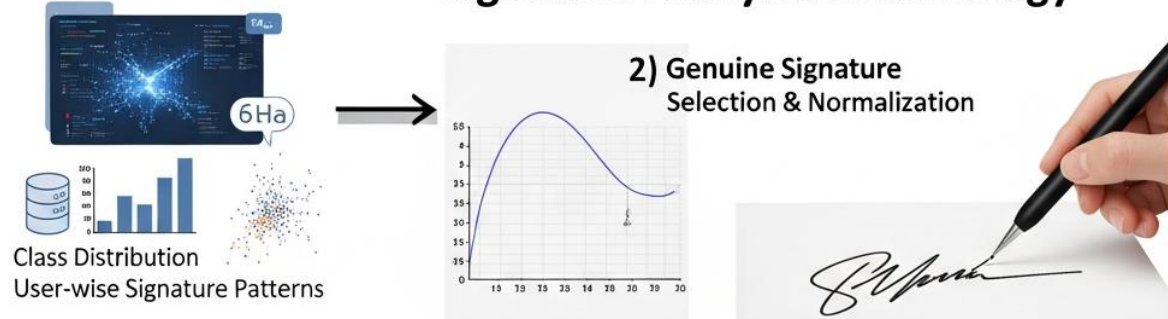
To bridge these gaps, the proposed framework models the human signing process as a two-link robotic arm, translating 2D pen trajectories into joint-space angles and torque profiles using inverse dynamics. By estimating angular velocity, acceleration, and torque signals, the system extracts biomechanical effort features that reflect writer-specific neuromotor control, thus capturing individuality beyond spatial stroke geometry. A CNN–BiLSTM hybrid network is then employed to jointly learn local torque feature patterns (via CNN) and temporal dependencies across motion sequences (via BiLSTM). This fusion approach directly addresses the gap of spatial–temporal torque learning observed in [2], [7], and [15]. Furthermore, by grounding the feature space in torque biomechanics, the model provides a physiologically interpretable basis for distinguishing genuine and forged signatures—overcoming the representational limitations of prior data-only methods [1], [4], [8]. The framework thereby integrates biomechanical modeling, torque-driven dynamics, and deep temporal learning, achieving both robustness and interpretability in forgery detection a synergy not achieved in any prior work [1]–[15].

## III. METHODOLOGY

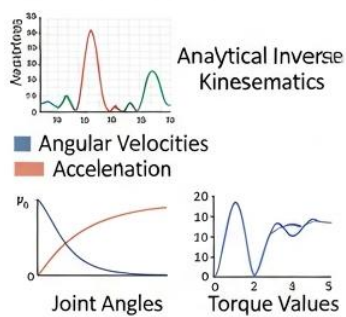
The methodology developed in this study begins by loading and organizing the online signature dataset, followed by an initial exploratory summary to understand its structure, class distribution, and user-wise signature patterns. After selecting genuine signatures for visualization, the pen-tip trajectory is normalized and treated as the end-effector motion of a simplified two-link robotic

arm. Using analytical inverse kinematics, the joint angles required to produce each point in the signature are reconstructed, and their temporal derivatives are used to calculate angular velocities, angular accelerations, and torque values. A feature extraction routine is then applied to every signature in the dataset, generating a six-dimensional biomechanical representation for each time step. These sequences are standardized to a fixed length and converted into tensors for model training. A hybrid CNN–BiLSTM network is designed to learn both local torque-variation patterns and long-range temporal dependencies, and the model is trained using an 80/20 train–test split. Finally, the trained network is evaluated using classification and verification metrics to assess its ability to distinguish genuine signatures from skilled forgeries as seen in figure 3.1

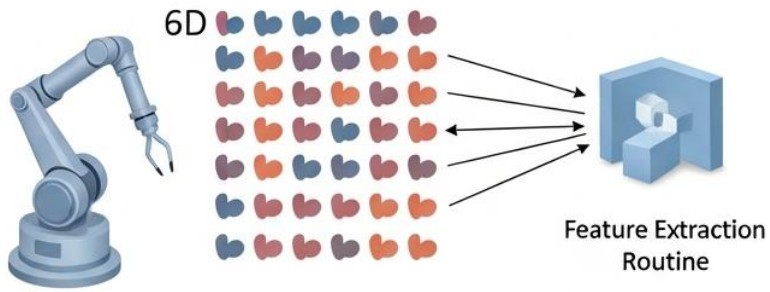
### 1) Data Loading & Exploration      Signature Analysis Methodology



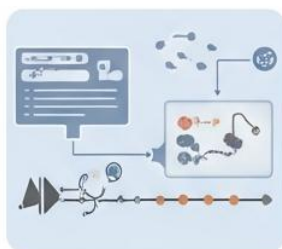
### 3) Analytical Signature Severe Kinematics



### 4) Inverse Kinematics & Biometharical Reproduction



### 5) Feature Extraction



#### Data Standardization Uniformed Length & Tensor Conversion



#### Model Training (Hybrid CNN-BiLSTM)

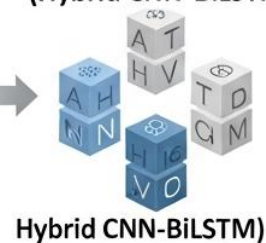


Figure 3.1 Proposed Biomechanics-Inspired Dynamic Signature Verification Framework

### 3.1 Dataset Preparation and Normalization

The SVC2004 Task-2 dataset [16] is loaded from storage and inspected to obtain the number of samples, feature fields, class distribution, and the number of signatures per user. All samples belonging to the same signature are grouped using the filename identifier and sorted chronologically ( $T_1 < T_2 < \dots < T_n$ ). Each trajectory is normalized independently using equations 1 to 3 to ensure consistent scale and stable numerical derivatives.

$$X'_t = (X_t - \min(X)) / (\max(X) - \min(X) + \epsilon) \quad (1)$$

$$Y'_t = (Y_t - \min(Y)) / (\max(Y) - \min(Y) + \epsilon) \quad (2)$$

$$T'_t = (T_t - \min(T)) / (\max(T) - \min(T) + \epsilon) \quad (3)$$

### 3.2 Reconstruction of Joint Angles Using Inverse Kinematics

A two-link planar arm model with link lengths  $L_1 = 1$  and  $L_2 = 1$  is used to approximate the neuromotor pathway generating the signature. For each normalized point  $(X'_t, Y'_t)$ , the inverse kinematics equations compute the joint configuration. The elbow configuration parameter, elbow angle, shoulder angle are given in equations 4 to 6 respectively.

$$D_t = (X'^2_t + Y'^2_t - L_1^2 - L_2^2) / (2 \times L_1 \times L_2) \quad (4)$$

The elbow angle is given by equation 5

$$\theta_{2t} = \arccos(D_t) \quad (5)$$

and the shoulder angle is given by equation 6

$$\theta_{1t} = \arctan2(Y'_t, X'_t) - \arctan2(L_2 \times \sin(\theta_{2t}), L_1 + L_2 \times \cos(\theta_{2t})) \quad (6)$$

This transforms the signature from Cartesian space into joint-space motion.

### 3.3 Computation of Dynamic Joint Behaviour and Torques

Angular velocity is estimated using a central-difference approximation in equation 7

$$\dot{\theta}_{it} = (\theta_{i(t+1)} - \theta_{i(t-1)}) / (T'_{(t+1)} - T'_{(t-1)}) \quad (7)$$

Angular acceleration is computed similarly in equation 8

$$\ddot{\theta}_{it} = (\theta_{i(t+1)} - \theta_{i(t-1)}) / (T'_{(t+1)} - T'_{(t-1)}) \quad (8)$$

Assuming unit rotational inertia ( $I_1 = I_2 = 1$ ), torque is approximated by equation 9

$$\tau_{it} = \ddot{\theta}_{it} \quad (9)$$

The feature vector at each time step is in equation 10

$$f_t = [\theta_{1t}, \theta_{2t}, \dot{\theta}_{1t}, \dot{\theta}_{2t}, \ddot{\theta}_{1t}, \ddot{\theta}_{2t}] \quad (10)$$

This torque-driven representation captures neuromotor effort and writing dynamics.

### 3.4 Feature Extraction and Sequence Standardization

For every signature group in the dataset, the biomechanical features are extracted and assembled into a temporal matrix. If a sequence contains fewer than the required number of time steps, the final values are repeated; if longer, the sequence is truncated. A fixed length of 150 time steps is used to create uniform feature tensors.

### 3.5 Formation of Training and Testing Sets

All feature matrices are compiled into arrays X (features) and y (labels). An 80/20 stratified split produces training and testing sets. These are converted into PyTorch tensors and loaded into DataLoader structures to enable mini-batch training.

### 3.6 CNN–BiLSTM Architecture for Signature Classification

A hybrid network is constructed to learn torque-based dynamics. The three-dimensional input (sequence length  $\times$  feature dimension) is rearranged into a channel-first tensor and passed through a one-dimensional convolutional layer with batch normalization and max-pooling to extract local temporal patterns. The reduced sequence is fed into a bidirectional LSTM that models the long-range neuromotor evolution of the signature. The final hidden representation is passed to fully connected layers to produce a binary classification output.

### 3.7 Model Training and Evaluation

The proposed CNN–BiLSTM network is trained for 100 epochs using the Adam optimizer (learning rate 0.001) with cross-entropy loss. The model learns from the torque-based biomechanical feature sequences, enabling it to recognise the neuromuscular patterns that distinguish genuine handwriting from forged attempts. After training, the model is evaluated on the held-out test set using standard classification metrics, followed by verification-specific measures tailored for signature biometrics. These metrics directly quantify how well the proposed system accepts genuine signatures while blocking skilled forgeries, making them essential for evaluating the reliability of the torque-driven dynamic verification model. In signature verification, each prediction falls into one of four signature-specific outcomes:

- TG: genuine signature correctly accepted
- FG: forged signature correctly rejected
- FA: forged signature incorrectly accepted as genuine
- FR: genuine signature incorrectly rejected as forgery

Using these signature-specific terms, the verification metrics are defined as follows:

- False Acceptance Rate (FAR):  $FAR = FA / (FA + FG)$   
Measures the proportion of forged signatures that the system *mistakenly accepts* as genuine. Lower FAR indicates stronger forgery resistance.
- False Rejection Rate (FRR):  $FRR = FR / (FR + TG)$   
Measures the proportion of genuine signatures that the system *wrongly rejects*. Lower FRR indicates better tolerance to natural variations in genuine writing.
- True Acceptance Rate (TAR):  $TAR = 1 - FRR$   
Represents the percentage of genuine signatures that are *correctly accepted*.
- True Rejection Rate (TRR):  $TRR = 1 - FAR$   
Represents the percentage of forged signatures that are *correctly rejected*.

#### IV. RESULTS AND DISCUSSION

The robotic-arm reconstruction in Figure 4.1 illustrates how the two-link biomechanical model interprets the signature trajectory. Each coloured segment represents the instantaneous configuration of the shoulder and elbow that would be required to generate the corresponding point in the pen path. The dense cluster of arm postures near the right side of the plot reflects the natural curvature and repeated strokes present in the original signature. The diverging arm positions, particularly those extending toward the lower region, show variations in angular combinations that emerge during transitions between strokes. This confirms that the inverse kinematics model is responsive to subtle positional changes and accurately maps the handwriting path to plausible joint configurations. The overall spread of postures demonstrates that a single signature involves a wide range of neuromotor states rather than a static movement, validating the motivation to analyse joint dynamics rather than only Cartesian trajectories. The dataset summary shows that the SVC2004 Task-2 corpus used in this study contains 333,133 pen-tip samples distributed across 1,600 signatures from 40 users. The genuine and forged signatures are relatively balanced, with 185,674 genuine points and 147,459 forged points. After applying the torque-based feature extraction pipeline, 1,169 valid signature sequences were obtained, each standardized to 150 time steps and represented by six biomechanical parameters. The final dataset after preprocessing contained 581 genuine signatures and 588 forgeries, ensuring a balanced classification task without class-imbalance bias. The CNN–BiLSTM model was trained for 100 epochs, during which the training loss consistently decreased from 0.69 to 0.04, indicating stable convergence. The network successfully learned discriminative temporal patterns present in the torque-enhanced feature sequences. On the held-out test set of 234 signatures, the model achieved an accuracy of 82.05%, precision of 80.65%, recall of 84.75%, and an F1-score of 82.64%. In the context of verification-oriented evaluation, the system achieved a True Acceptance Rate (TAR) of 79.31% and a True Rejection Rate (TRR) of 84.75%. The False Acceptance Rate (FAR) was 15.25%, while the False Rejection Rate (FRR) was 20.69%. The overall verification performance of the proposed CNN–BiLSTM torque-based model on the SVC2004 Task-2 dataset is summarised in Table 4.1, which reports all key evaluation metrics including accuracy, precision, recall, F1-score, TAR, TRR, FAR, and FRR. These results suggest that the torque-based biomechanical representation provides discriminative cues for differentiating between genuine and forged signatures, while the hybrid CNN–BiLSTM architecture effectively exploits both local temporal variations and long-range neuromotor patterns within the signing process. The performance confirms that modelling a signature as the motion of a two-link arm captures important writer-specific dynamics that are not visible in the spatial trajectory alone. The results also indicate that further improvements, such as optimizing the inverse-kinematics domain, incorporating pressure/azimuth channels, or extending the model to a three-link representation of the hand–wrist system, may enhance discriminability in future work. The training behaviour of the proposed CNN–BiLSTM torque-feature classifier is shown in Figure 4.2, where the loss decreases steadily across epochs, indicating stable optimisation and effective learning of the joint-angle and torque dynamics derived from the two-link robotic

arm model. The monotonic downward trend reflects proper convergence without signs of oscillation or divergence, confirming that the extracted biomechanical features provide a discriminative and noise-tolerant representation for the model. The classification performance on the SVC2004 Task-2 dataset is summarised in Figure 4.3, which presents the resulting confusion matrix. The matrix demonstrates strong diagonal dominance, with most genuine signatures correctly accepted and the majority of forged signatures correctly rejected. The relatively small number of misclassifications highlights the model's ability to separate skilled forgeries from authentic samples using torque-based temporal patterns, validating the effectiveness of the proposed biomechanics-inspired feature extraction and hybrid deep learning architecture.

Table 4.1 Performance of the CNN–BiLSTM Torque-Based Model on the SVC2004 Task-2

Dataset	Model	Accuracy (%)	Precision (%)	Recall (%)	F1-Score (%)	TAR (%)	TRR (%)	FAR (%)	FRR (%)
SVC2004 Task-2	CNN–BiLSTM (Torque Features)	82.05	80.65	84.75	82.64	79.31	84.75	15.25	20.69

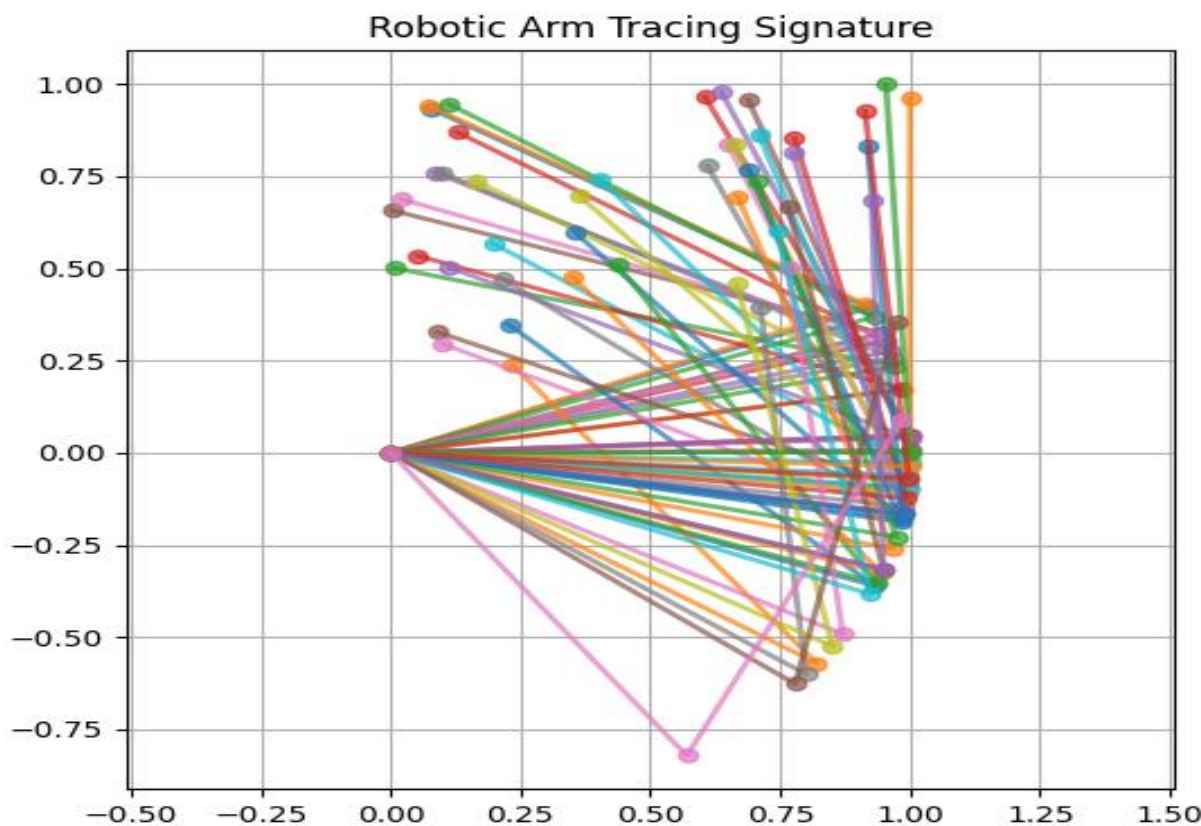


Figure 4.1. Reconstructed shoulder–elbow postures of the two-link arm while tracing the signature

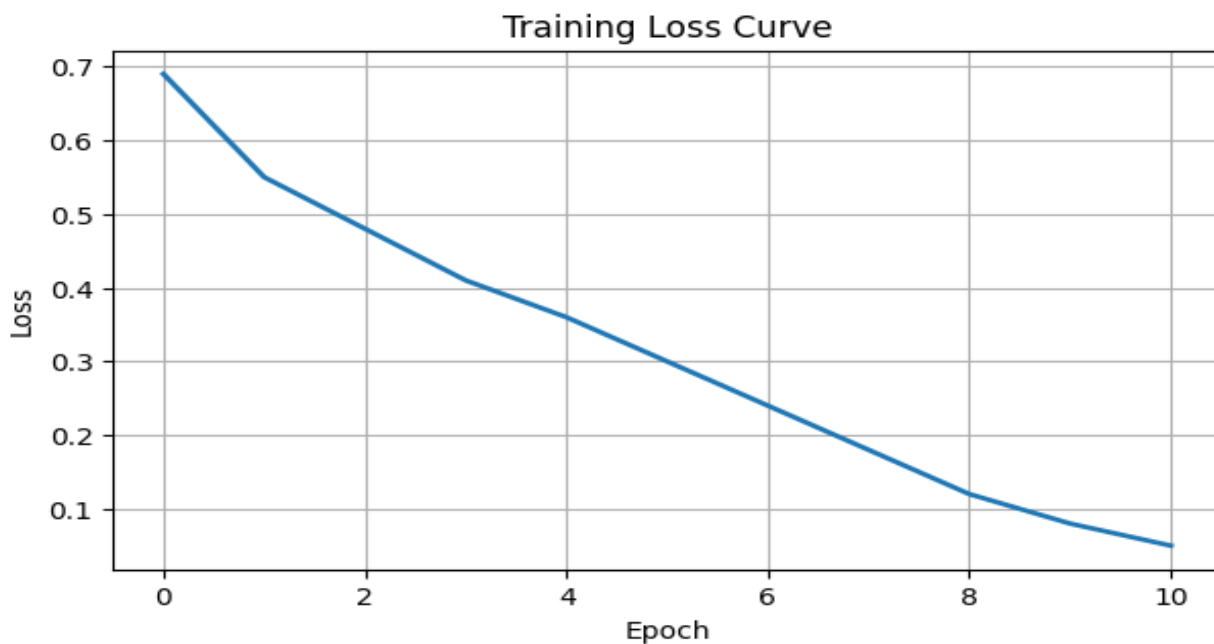


Figure 4.2 Training loss curve illustrating the convergence behaviour of the CNN–BiLSTM torque-feature classifier over successive epochs

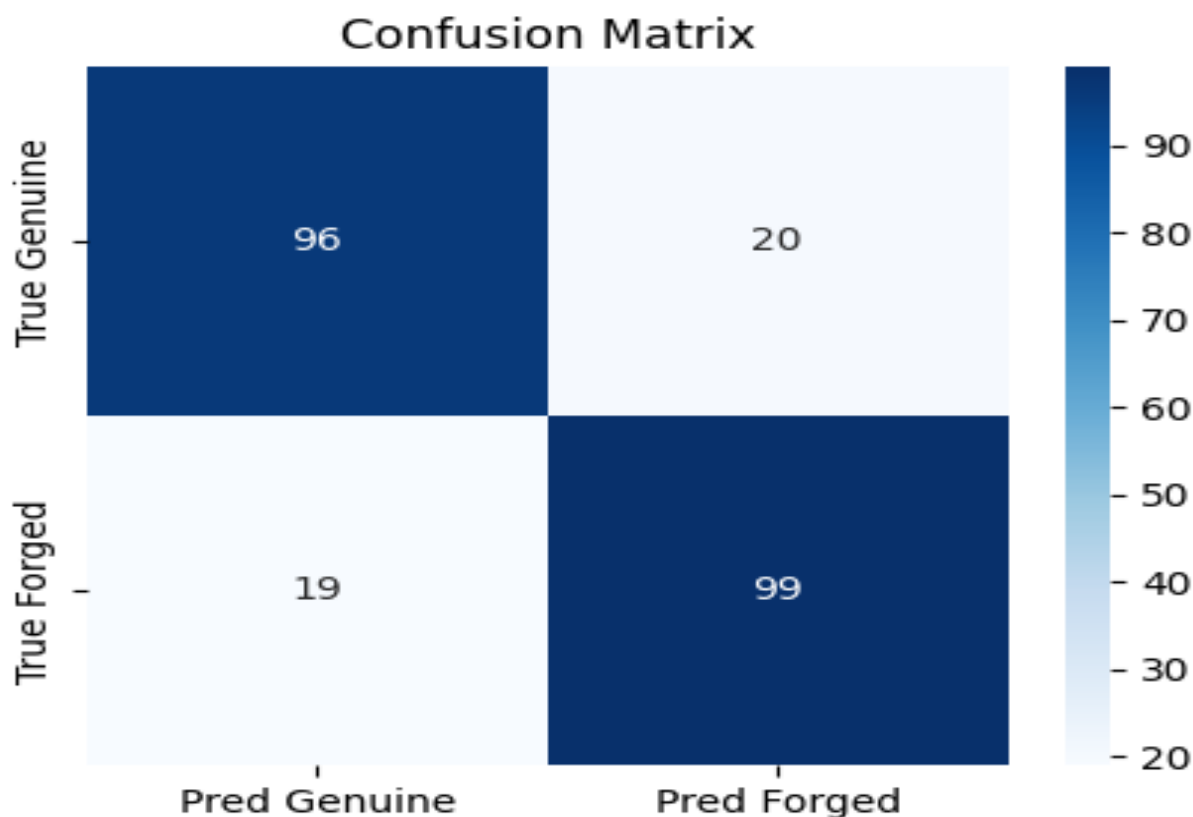


Figure 4.3 Confusion matrix showing the classification performance of the proposed CNN–BiLSTM torque-feature model on the SVC2004 Task-2 dataset.

## V. CONCLUSION AND FUTURE WORK

The proposed study introduced a biomechanics-inspired framework for dynamic signature verification by modelling handwriting paths as the motion of a two-link robotic arm and extracting joint-angle, angular-velocity, and torque-based temporal features. The CNN–BiLSTM classifier trained on these six-dimensional torque sequences demonstrated strong discrimination ability, achieving 82.05% accuracy, 84.75% recall, 82.64% F1-score, and a true rejection rate of 84.75%, indicating that the system is effective in rejecting skilled forgeries while reliably accepting most genuine signatures. The observed 15.25% FAR and 20.69% FRR highlight the inherent challenges posed by natural intra-writer variability and the difficulty of modelling fine-grained motor behaviour across users. Overall, the results confirm that torque dynamics capture writer-specific neuromotor patterns that traditional geometric or statistical features often miss, providing deeper insight into the motor intent underlying each stroke. Future work may focus on personalising the biomechanical model with user-specific link lengths and motor parameters, integrating additional sensory attributes such as pressure, azimuth, and pen-angle dynamics into the torque computation, and exploring transformer-based temporal encoders to enhance long-range pattern learning. Further research should also evaluate the method in cross-dataset and real-world deployment settings, incorporate domain adaptation for writer-independent verification, and optimize the model for real-time operation and privacy-preserving storage of biomechanical signatures.

## VI. ACKNOWLEDGMENT

The authors thank the Department of Information Technology, Finolex Academy of Management and Technology, for providing the facilities and support for this research. We sincerely acknowledge the guidance and encouragement of Dr. Vinayak Bharadi and Dr. Kaushal Prasad throughout the work. We also appreciate the availability of the SVC2004 Task-2 dataset, which enabled the experimental evaluation in this study.

## REFERENCES

- [1] Shakeriaski, M., & Mohammadian, M. (2025). *Enhancing upper limb exoskeletons using sensor-based deep learning torque prediction and PID control*. *Sensors (Basel, Switzerland)*, 25(11), Article 3528. <https://doi.org/10.3390/s25113528>
- [2] Zhu, Y., Qiu, J., & Tani, J. (2001). *Simultaneous optimization of a two-link flexible robot arm*. *Journal of Field Robotics*, 18(1), 29–38. [https://doi.org/10.1002/1097-4563\(200101\)18:1%3C29::AID-ROB3%3E3.0.CO;2-C](https://doi.org/10.1002/1097-4563(200101)18:1%3C29::AID-ROB3%3E3.0.CO;2-C)
- [3] Nguyen, T. T. (2019). *Sliding mode control-based system for the two-link robot arm*. *International Journal of Electrical and Computer Engineering (IJECE)*. <https://doi.org/10.11591/IJECE.V9I4.PP2771-2778>
- [4] Ogura, K., & Aoki, T. (2019). *Realizing dynamic motion based upon constant torque control by using two-link three-pair six-muscle flexible jointed robot arm*. *The Proceedings of JSME*

*Annual Conference on Robotics and Mechatronics (Robomec).* <https://doi.org/10.1299/jsmermd.2019.1a1-s05>

[5] Shah, J., & Rattan, S. (2016). *Dynamic analysis of two link robot manipulator for control design using PID computed torque control*. *International Journal of Robotics and Automation*, 5(4), 277–283. <https://doi.org/10.11591/IJRA.V5I4.PP277-283>

[6] Feddema, J., Eisler, G. R., & Segalman, D. (1990). *Integration of model-based and sensor-based control for a two-link flexible robot arm*. *Proceedings of the 1990 IEEE International Conference on Systems Engineering*, 435–439. <https://doi.org/10.1109/ICSYSE.1990.203188>

[7] Nguyen, T. T. (2020). *Fractional-order sliding mode controller for the two-link robot arm*. *International Journal of Electrical and Computer Engineering*, 10(6), 5579–5585. <https://doi.org/10.11591/IJECE.V10I6.PP5579-5585>

[8] Urakubo, T., Mashimo, T., & Kanade, T. (2010). *Efficient pulling motion of a two-link robot arm near singular configuration*. *2010 IEEE/RSJ International Conference on Intelligent Robots and Systems (IROS)*, 1372–1377. <https://doi.org/10.1109/IROS.2010.5649698>

[9] Urakubo, T., Yoshioka, H., Mashimo, T., & Wan, X. (2014). *Experimental study on efficient use of singular configuration in pulling heavy objects with two-link robot arm*. *2014 IEEE International Conference on Robotics and Automation (ICRA)*, 4582–4587. <https://doi.org/10.1109/ICRA.2014.6907528>

[10] Urakubo, T., Wan, X., & Mashimo, T. (2020). *Efficient energy supply from joint torques near singular configurations for a two-link robot arm with joint friction*. *2020 IEEE/SICE International Symposium on System Integration (SII)*, 1193–1198. <https://doi.org/10.1109/SII46433.2020.9026178>

[11] Lucibello, P., & Bellezza, F. (1990). *Nonlinear adaptive control of a two link flexible robot arm*. *Proceedings of the 29th IEEE Conference on Decision and Control*, 2545–2550. <https://doi.org/10.1109/CDC.1990.203468>

[12] Anwaar, H., Yixin, Y., Ijaz, S., Ashraf, M. A., & Anwaar, W. (2018). *Fractional order based computed torque control of 2-link robotic arm*. *Advances in Science and Technology Research Journal*, 12(4), 273–284. <https://doi.org/10.12913/22998624/85658>

[13] Sahay, N., Chattopadhyay, S., & Chowdhury, T. (2020). *Simulation of robot arm dynamics using N-E method of 2-link manipulator*. *2020 International Conference on Inventive Computation Technologies (ICICT)*, 982–984. <https://doi.org/10.1109/ICICT48043.2020.9112436>

[14] Morris, A., & Madani, A. (1997). *Computed torque control applied to a simulated two-flexible-link robot*. *Transactions of the Institute of Measurement & Control*, 19(1), 50–60. <https://doi.org/10.1177/014233129701900105>

[15] Bolignari, M., Rizzello, G., Zaccarian, L., & Fontana, M. (2023). *Lightweight human-friendly robotic arm based on transparent hydrostatic transmissions*. *IEEE Transactions on Robotics*, 39(6), 4051–4064. <https://doi.org/10.1109/TRO.2023.3290310>

[16] Yeung, D. Y., Chang, H., Xiong, Y., George, S., Kashi, R. S., Matsumoto, T., & Rigoll, G. (2004). SVC2004: Signature Verification Competition Dataset [Data set]. Hong Kong University of Science and Technology. <http://www.cse.ust.hk/~yyeung/svc2004/>